

Main Chain Liquid Crystalline Polytriazoles with Aggregation-Induced Emission Characteristics: Click polymerization, Mesomorphic Packing, and Solid State Emission

Wang Zhang Yuan^a, Zhen Qiang Yu^b, Jacky Wing Yip Lam^a, Cathy K. W. Jim^a, Ben Zhong Tang^{*,a,c}

^aDepartment of Chemistry, The Hong Kong University of Science & Technology, Clear Water Bay, Kowloon, Hong Kong, China

^bSchool of Chemistry and Chemical Engineering, Shenzhen University, Shenzhen 518060, China,

^cDepartment of Polymer Science & Engineering, Zhejiang University, Hangzhou, Zhejiang 310027, China

ABSTRACT

Biphenyl-containing diazides and diynes carrying tetraphenylethylene units are designed and synthesized. Their “click” polymerizations are initiated by Cu(PPh₃)₃Br in THF or DMF, affording soluble, regioregular polytriazoles in high yields (up to 94.8%) with narrow molecular weight distributions. The structures and properties of the polymers are evaluated and characterized by IR, NMR, UV, PL, TGA, DSC, POM and XRD measurements. All the polymers are almost nonluminescent when dissolved in solutions but become highly emissive when aggregated in poor solvents or fabricated as thin films in the solid state, displaying a novel phenomenon of aggregation-induced emission. The photophysical properties of the polymers are sensitive to their molecular structures and their solid-state quantum yields decrease with an increase in the spacer length. All the polymers enjoy high thermal stability, with 5% weight loss occurring at temperatures up to 406 °C. They are mesomorphic. While polymers with rigid main chains exhibit nematicity, those with longer spacer lengths show better mesogenic packing and hence form smectic phases at higher temperatures.

Keywords: polytriazoles, click polymerization, aggregation-induced emission, liquid crystalline polymers

1. INTRODUCTION

Liquid crystals (LCs) are materials lying between liquids and crystals. They are fluids but show birefringence.¹ Such unique properties thus enable them to find a wide range of high-tech applications.² For examples, they are widely used in panel display devices because of their anisotropic nature and responsiveness to electric fields.^{2,3} While ferroelectric LCs are used as temperature⁴ and pressure sensors⁵, and are promising non-linear optical materials⁶, liquid crystalline semiconductors have favored potential applications in field-effect transistors,⁷ photovoltaic cells,⁸ and light-emitting diodes.⁹ Furthermore, dynamic and anisotropic liquid crystalline structures can work as low-dimensional charge-¹⁰, ion-¹¹, and mass-transporting¹² materials.

There are growing interests in fluorescent LCs in the past decades.^{9,13-15} The combination of intrinsic light-emitting capability and unique supramolecular organization feature within a liquid crystalline phase is of fundamental interests for applications such as anisotropic light-emitting diodes and emissive liquid crystal displays.^{9,16,17} The fluorescent LCs may emit linear or circular polarized light when aligned,^{9,13g,15,17} which may be utilized for the construction of lighting and orientating layers in liquid crystal optical display devices, thus obviating the use of backlight lamps, polyimide films, and polarizing sheets. The color and brightness of the light emitted by the liquid crystalline luminogens may be manipulated by external fields, which may lead to the development of readily tunable electrochromic and optical switching systems. Such approach can simplify the device design and substantially increase the device brightness, contrast, efficiency, and viewing angle.^{3,18}

* Corresponding authors: B. Z. Tang (E-mail: tangbenz@ust.hk. Tel. +852-2358-7375. Fax. +852-2358-1594).

Despite the promising prospects of fluorescent LCs, their synthesis is challenging. In the mesophases, particularly those formed by disc liquid crystals,^{13c} the chromophoric mesogens are packed orderly and experience strong intermolecular interactions, which often quench their light emissions due to the formation of detrimental species such as excimers.^{13g,19-21} The light emission is often enhanced at the expense of molecular packing, thus making the synthesis of mesomorphic materials with efficient light emissions a daunting job.

Our group is interested in creating low molecular weight and polymeric liquid crystals.²² We have synthesized a wide variety of side chain liquid crystalline polyacetylenes carrying chromophoric and mesogenic pendants. Some of which can emit intensely in the condensed phase.^{23,24} Recently, we discovered a novel phenomenon of aggregation-induced emission (AIE) in some propeller-shaped molecules.^{25,26} Instead of quenching commonly observed in “conventional” luminophors, aggregation has enhanced their light emission, turning them from weak fluorophors into strong emitters. Introduction of AIE-active dyes into liquid crystals may solve such the above problem but such attempt has rarely reported.

Tetraphenylethylene (TPE) is a typical AIE-active dye.^{26,27} It is nonemissive in dilute solution because its active intramolecular rotations effectively dissipates the energy of its excitons through nonradiative pathways. On the contrary, it emits intensely in the aggregate state due to the physical restriction of its intramolecular rotations. Polymers containing TPE units are thus expected to show AIE phenomenon.²⁸ Meanwhile, the polymers can be imparted with mesomorphic properties through rational molecular design. Herein, we present our effort on the creation of AIE-active liquid crystalline polymers. The copper-catalyzed 1,3-dipolar cycloaddition of alkynes with azides is a typical example of “click reaction”. Since the reaction enjoys the advantages of mild reaction conditions, high efficiency and regioselectivity, and simple purification procedures, it has become a versatile synthetic tool with applicability in diverse areas.²⁹⁻³¹ In this paper we adopted such methodology for the preparation of new polymers. All the synthesized polytriazoles are both AIE-active and liquid crystalline. Their solid-state quantum efficiencies range from 24.5 to 63.7%, which are much higher than those of reported luminescent liquid crystals.^{15b,20} The effects of spacer length on their emission efficiency and mesomorphic behaviors are also discussed.

2. EXPERIMENTAL

2.1 Materials

THF was distilled under normal pressure from sodium benzophenone ketyl under nitrogen immediately prior to use. Dichloromethane (DCM) was distilled under normal pressure over calcium hydride under nitrogen before use. Triethylamine (TEA) was distilled and dried over potassium hydroxide. *p*-Toluenesulfonic acid monohydrate (TsOH), *N,N'*-dicyclohexylcarbodiimide (DCC), 4-dimethylaminopyridine (DMAP), 6-bromohexanoic acid [7(5)], 11-bromoundecanoic acid [7(10)], 4,4'-biphenol (**8**), 4-bromobenzophenone (**10**), (trimethylsilyl)acetylene (**11**), 4-hydroxybenzophenone (**14**), copper(I) iodide (CuI), triphenylphosphine (PPh₃), dichlorobis(triphenylphosphine)palladium(II) [Pd(PPh₃)₃Cl₂], titanium tetrachloride (TiCl₄), zinc dust, 1 M tetrabutylammonium fluoride (TBAF) in THF (containing 5% water) were all purchased from Aldrich and used as received. Catalysts Cu(PPh₃)₃Br and Cp^{*}Ru(PPh₃)₂Cl were prepared according to the literature methods.³²

2.2 Instrumentation

¹H and ¹³C NMR spectra were measured on a Bruker ARX 400 spectrometer using chloroform-*d* or DMSO-*d*₆ as solvent and tetramethylsilane (TMS) as internal standard. Matrix-assisted laser desorption/ionization time-of-flight (MALDI-TOF) high-resolution mass spectra (HRMS) were recorded on a GCT premier CAB048 mass spectrometer. Absorption spectra were taken on a Milton Roy Spectronic 3000 Array spectrometer. Emission spectra were taken on a Perkin-Elmer spectrofluorometer LS 55. Molecular weights (*M_w* and *M_n*) and polydispersity indexes (*M_w*/*M_n*) of the polymers were estimated by a Waters Associates gel permeation chromatography (GPC) system in THF. A set of monodisperse polystyrene standards covering molecular weight range of 10³–10⁷ was used for the molecular weight calibration.

The thermal stability of the polymers was evaluated on a Perkin-Elmer TGA 7 under nitrogen at a heating rate of 20 °C/min. A Perkin-Elmer DSC 7 was employed to measure the phase transition thermograms. An Olympus BX 60 polarized optical microscope (POM) equipped with a Linkam TMS 92 hot stage was used to observe the anisotropic optical textures. One-dimensional wide-angle X-ray diffraction (1D-WAXD) powder experiments were performed on a

Philips X'Pert Pro diffractometer with a 3 kW ceramic tube as the X-ray source (Cu K α) and an X'celerator detector. The sample stage was set horizontally and the samples were protected by nitrogen gas during the measurements. The reflection peak positions were calibrated with silicon powder ($2\theta > 15^\circ$) and silver behenate ($2\theta < 10^\circ$). Background scattering was recorded and subtracted from the sample patterns. A temperature control unit (Paar Physica TCU 100) in conjunction with the diffractometer was utilized to study the structure evolutions as a function of temperature.

2.3 Monomer Preparation

The synthetic routes to monomers **1(x)** are given in Scheme 1. The experimental procedures are given below.

5-Bromopentyl 4,4'-biphenyldicarboxylate [9(5)]. Into a 250 mL round-bottom flask were placed 2.34 g (12 mmol) of **7(5)**, 1.12 g (6 mmol) of **8**, 3.71 g (18 mmol) of DCC, 293 mg (2.4 mmol) of DMAP, and 457 mg (2.4 mmol) of TsOH in 150 mL THF. The resultant mixture was stirred at room temperature for 24 h. After filtering the formed urea, the solid was washed with THF and the filtrate was concentrated by a rotary evaporator. The product was purified by a silica gel column using a mixture of chloroform/hexane (1:1 by volume) as eluent. White solid, yield 86.2% (2.79 g). ^1H NMR (400 MHz, CDCl_3), δ (TMS, ppm): 7.54 (d, 4H, aromatic protons meta to OCO-), 7.16 (m, 4H, aromatic protons ortho to OCO-), 3.45 (t, 4H, CH_2Br), 2.61 (t, 4H, OCOCH_2), 1.94 (m, 4H, $\text{CH}_2\text{CH}_2\text{Br}$), 1.81 (m, 4H, $\text{OCOCH}_2\text{CH}_2$), 1.60 (m, 4H, $\text{CH}_2\text{CH}_2\text{CH}_2\text{Br}$). ^{13}C NMR (100 MHz, CDCl_3), δ (TMS, ppm): 171.94 (C=O), 150.12 (aromatic carbons connected to OCO-), 138.08 (aromatic carbons para to OCO-), 128.12 (aromatic carbons meta to OCO-), 121.86 (aromatic carbons ortho to OCO-), 34.14 (CH_2Br), 33.42 (OCOCH_2), 32.34 ($\text{CH}_2\text{CH}_2\text{Br}$), 27.59 ($\text{CH}_2\text{CH}_2\text{CH}_2\text{Br}$), 24.04 ($\text{OCOCH}_2\text{CH}_2$).

10-Bromodecyl 4,4'-biphenyldicarboxylate [9(10)]. The synthetic procedures are similar to those of **9(5)** described above. White solid, yield 79.2%. ^1H NMR (400 MHz, CDCl_3), δ (TMS, ppm): 7.54 (d, 4H, aromatic protons meta to OCO-), 7.15 (d, 4H, aromatic protons ortho to OCO-), 3.41 (t, 4H, CH_2Br), 2.58 (t, 4H, OCOCH_2), 1.84 (m, 4H, $\text{CH}_2\text{CH}_2\text{Br}$), 1.77 (m, 4H, $\text{OCOCH}_2\text{CH}_2$), 1.32 ~ 1.43 [m, 12H, $\text{CH}_2(\text{CH}_2)_6\text{CH}_2$]. ^{13}C NMR (100 MHz, CDCl_3), δ (TMS, ppm): 172.45 (C=O), 150.15 (aromatic carbons connected to OCO-), 138.12 (aromatic carbons para to OCO-), 128.11 (aromatic carbons meta to OCO-), 121.89 (aromatic carbons ortho to OCO-), 34.40 (CH_2Br), 34.05 (OCOCH_2), 32.82 ($\text{CH}_2\text{CH}_2\text{Br}$), 29.34, 29.31, 29.19, 29.07, 28.72, 28.14 [$(\text{CH}_2)_6\text{CH}_2\text{CH}_2\text{Br}$], 24.93 ($\text{OCOCH}_2\text{CH}_2$).

5-Azidopentyl 4,4'-biphenyldicarboxylate [1(5)]. Into a 250 mL round-bottom flask were placed 1.62 g (3 mmol) of **9(5)** and 507 mg (7.8 mmol) of NaN_3 . Then 80 mL of DMSO was added. After stirring at room temperature for 24 h, water was added. The mixture was extracted by DCM three times. The organic layers were combined, washed with brine, and dried over 5 g of Na_2SO_4 overnight. After filtration and solvent evaporation, the crude product was purified by a silica gel column using a chloroform/hexane mixture (1:1 by volume). White solid, yield 85.1%. IR (KBr), ν (cm^{-1}): 2096 (N_3 stretching), 1753 (C=O stretching). ^1H NMR (400 MHz, $\text{DMSO}-d_6$), δ (TMS, ppm): 7.66 (d, 4H, aromatic protons meta to OCO-), 7.20 (d, 4H, aromatic protons ortho to OCO-), 3.33 (t, 4H, CH_2N_3), 2.59 (t, 4H, OCOCH_2), 1.66 (m, 4H, $\text{CH}_2\text{CH}_2\text{N}_3$), 1.57 (m, 4H, $\text{OCOCH}_2\text{CH}_2$), 1.41 (m, 4H, $\text{CH}_2\text{CH}_2\text{CH}_2\text{N}_3$). ^{13}C NMR (100 MHz, $\text{DMSO}-d_6$), δ (TMS, ppm): 171.61 (C=O), 149.84 (aromatic carbons connected to OCO-), 136.75 (aromatic carbons para to OCO-), 127.58 (aromatic carbons meta to OCO-), 122.12 (aromatic carbons ortho to OCO-), 50.31 (CH_2N_3), 33.15 (OCOCH_2), 27.74 ($\text{CH}_2\text{CH}_2\text{N}_3$), 25.37 ($\text{CH}_2\text{CH}_2\text{CH}_2\text{N}_3$), 23.68 ($\text{OCOCH}_2\text{CH}_2$). HRMS (MALDI-TOF): m/e 487.2950 [$(\text{M}+\text{Na})^+$, calcd 487.2172].

10-Azidodecyl 4,4'-biphenyldicarboxylate [1(10)]. The synthetic procedures are similar to those of **1(5)** described above. However, due to the poor solubility of **9(10)** in DMSO at room temperature, the reaction mixture was carried out at 40°C . White solid, yield 89.3%. IR (KBr), ν (cm^{-1}): 2119 (N_3 stretching), 1747 (C=O stretching). ^1H NMR (400 MHz, CDCl_3), δ (TMS, ppm): 7.54 (d, 4H, aromatic protons meta to OCO-), 7.15 (d, 4H, aromatic protons ortho to OCO-), 3.26 (t, 4H, CH_2N_3), 2.58 (t, 4H, OCOCH_2), 1.77 (m, 4H, $\text{CH}_2\text{CH}_2\text{N}_3$), 1.60 (m, 4H, $\text{OCOCH}_2\text{CH}_2$), 1.31 [m, 24H, $(\text{CH}_2)_6$]. ^{13}C NMR (100 MHz, CDCl_3), δ (TMS, ppm): 172.34 (C=O), 150.22 (aromatic carbons connected to OCO-), 138.06 (aromatic carbons para to OCO-), 128.10 (aromatic carbons meta to OCO-), 121.89 (aromatic carbons ortho to OCO-), 51.49 (CH_2N_3), 34.41 (OCOCH_2), 29.39, 29.32, 29.20, 29.11, 29.08, 29.83 [$(\text{CH}_2)_6$], 26.70 ($\text{CH}_2\text{CH}_2\text{CH}_2\text{N}_3$), 24.93 ($\text{OCOCH}_2\text{CH}_2$). HRMS (MALDI-TOF): m/e 627.4815 [$(\text{M}+\text{Na})^+$, calcd 627.3737].

4-(Trimethylsilylethynyl)benzophenone (12). Into a 100 mL two-necked flask were added 70.1 mg (0.1 mmol) of $\text{Pd}(\text{PPh}_3)_2\text{Cl}_2$, 19 mg (0.1 mmol) of CuI , 13 mg (0.05 mmol) of PPh_3 , 1.3 g (5 mmol) of **10**, and a mixture of 55 mL of THF/TEA (5:50 v/v) under nitrogen. Then 0.9 mL (6.5 mmol) of (trimethylsilyl)acetylene (**11**) was injected into the flask and the mixture was stirred at 50°C for 24 h. The formed solid was removed by filtration and washed with diethyl ether.

The filtrate was concentrated by a rotary evaporator. The crude product was purified on a silica-gel column with chloroform/hexane (1:1 by volume) as eluent. Pale brown solid, yield 85.5%. IR (KBr), ν (cm^{-1}): 2158 (m, $\text{C}\equiv\text{C}$ stretching), 1649 (vs, $\text{C}=\text{O}$ stretching). ^1H NMR (400 MHz, CDCl_3), δ (TMS, ppm): 7.78, 7.76, 7.74, 7.57, 7.55, 7.48 (m, 9H, aromatic protons), 0.27 [s, 9H, $\text{Si}(\text{CH}_3)_3$]. ^{13}C NMR (100 MHz, CDCl_3), δ (TMS, ppm): 195.93 ($\text{C}=\text{O}$), 137.38, 136.97, 132.53, 131.77, 129.94, 129.88, 128.34, 127.33, 104.06 ($\text{Ar}-\text{C}\equiv$), 97.83 ($\text{Si}-\text{C}\equiv$), -0.17 [$-\text{Si}(\text{CH}_3)_3$]. HRMS (MALDI-TOF): m/e 277.1853 [$(\text{M}-\text{H})^+$, calcd 277.1127].

1,2-bis(4-trimethylsilylethynylphenyl)-1,2-diphenylethene (13). Into a 250 mL two-necked round-bottom flask with a reflux condenser were placed 1.18 g (18 mmol) of zinc dust, 4.18 g (15 mmol) of **12**. The flask was evacuated under vacuum and flushed with dry nitrogen for three times. Then 100 mL of THF was added. The mixture was cooled to $0-5^\circ\text{C}$, and 1 mL (9 mmol) of TiCl_4 was slowly added. The mixture was slowly warmed to room temperature, stirred for 0.5 h, and then refluxed overnight. The reaction was quenched with 10% K_2CO_3 aqueous solution, and large amount of water was added until the solid turned to grey or white. The mixture was extracted with DCM for three times and the collected organic layer was washed by brine twice. Then mixture was dried over 5 g of anhydrous sodium sulfate for 4 h. The crude product was condensed and purified on a silica-gel column using chloroform/hexane (1:5 by volume) as eluent. Light yellow solid, yield 90.2%. IR (KBr), ν (cm^{-1}): 2156 ($\text{C}\equiv\text{C}$ stretching). ^1H NMR (400 MHz, CDCl_3), δ (TMS, ppm): 7.24, 7.22, 7.20, 7.13, 7.12, 7.11, 7.10, 7.01, 7.00, 6.99, 6.97, 6.96, 6.95, 6.94 (18H, aromatic protons), 0.23, 0.25 [s, 18H, $\text{Si}(\text{CH}_3)_3$]. ^{13}C NMR (100 MHz, CDCl_3), δ (TMS, ppm): 143.95, 143.83, 143.01, 142.97, 140.90, 131.46, 131.35, 131.31, 131.19, 127.89, 127.74, 126.84, 126.75, 121.21, 121.04, 105.28, 105.11 ($\text{Ar}-\text{C}\equiv$), 94.59 and 94.42 ($\text{Si}-\text{C}\equiv$), -0.04 [$-\text{Si}(\text{CH}_3)_3$].

1,2-bis(4-ethynylphenyl)-1,2-diphenylethene (2). Into a 100 mL round bottom flask was placed 40 mL of THF solution of **13** (1.57 g, 3 mmol) followed by 12 mL of 1 M tetrabutylammonium fluoride in THF. After stirring for 45 min, 40 mL of water was added and the mixture was extracted by 200 mL of DCM three times. The DCM solution was washed by brine twice and then dried over 5 g of anhydrous Na_2SO_4 for 2 h. The crude product was condensed and purified on a silica-gel column using a mixture of chloroform/hexane (1:5 by volume) as eluent. Light yellow solid, yield 92.1%. IR (KBr), ν (cm^{-1}): 3276 ($\text{HC}\equiv$ stretching), 2107 ($\text{C}\equiv\text{C}$ stretching). ^1H NMR (400 MHz, $\text{DMSO}-d_6$), δ (TMS, ppm): 7.25, 7.23, 7.22, 7.20, 7.15, 7.11, 7.14, 7.12, 7.10, 7.09, 6.96, 6.93, 6.92 (18 H, aromatic protons), 4.13 and 4.11 (two singlet, $\text{HC}\equiv$). ^{13}C NMR (100 MHz, $\text{DMSO}-d_6$), δ (TMS, ppm): 143.39, 143.37, 142.26, 142.19, 140.35, 131.14, 131.02, 130.76, 130.70, 130.46, 130.42, 127.89, 127.77, 126.83, 126.71, 119.78, 119.66, 83.14 ($\text{Ar}-\text{C}\equiv$), 80.97 and 80.88 ($\equiv\text{CH}$). HRMS (MALDI-TOF): m/e 380.1231 [$(\text{M})^+$, calcd 380.1565].

1,2-bis(4-hydroxyphenyl)-1,2-diphenylethene (15). The synthetic procedures are similar to those of **13** described above. White Solid, yield 90.2%. ^1H NMR (400 MHz, CDCl_3), δ (TMS, ppm): 7.03–7.12 (m, 10H), 6.90 (t, 4H), 6.57 (d, 4H). ^{13}C NMR (100 MHz, CDCl_3), δ (TMS, ppm): 154.13 (aromatic carbons connected to OH), 144.21, 139.67, 135.53, 132.79, 131.50, 127.76, 126.36, 114.72.

1,2-bis(1,4-phenylene)-1,2-diphenylvinyl bis(6-hexynoate) [3(3)]. Into a 250 mL one-necked round-bottom flask were placed 1.82 g (5 mmol) of **15**, 1.23 g (11 mmol) of 5-hexynoic acid **16(3)**, 2.48 g (12 mmol) of DCC, 244.3 mg (2 mmol) of DMAP, and 380.4 mg (2 mmol) of TsOH in 100 mL of DCM. The resultant mixture was stirred for 24 h at room temperature. After filtering the formed urea, the solid was washed with DCM and the filtrate was concentrated by a rotary evaporator. The product was purified by a silica gel column using a mixture of chloroform/hexane (1:1 v/v) as eluent. A white solid of **3(3)** was obtained in 85.9% yield. IR (KBr), ν (cm^{-1}): 3296 ($\text{HC}\equiv$ stretching), 2118 ($\text{C}\equiv\text{C}$ stretching), 1756 ($\text{C}=\text{O}$ stretching). ^1H NMR (400 MHz, $\text{DMSO}-d_6$), δ (TMS, ppm): 7.15, 7.13, 7.12, 7.10, 6.99, 6.97, 6.95, 6.92, 6.89, 6.87 (18H, aromatic protons), 2.81 (t, 2H, $\text{HC}\equiv$), 2.60 (m, 4H, OCOCH_2), 2.24 (m, 4H, $\equiv\text{CCH}_2$), 1.76 (m, 4H, $\text{OCOCH}_2\text{CH}_2$). ^{13}C NMR (100 MHz, $\text{DMSO}-d_6$), δ (TMS, ppm): 170.89 ($\text{C}=\text{O}$), 148.65, 148.61, 142.74, 142.69, 140.33, 140.27, 139.83, 131.42, 130.43, 127.78, 127.70, 126.65, 126.48, 121.06, 120.97, 83.41 ($\equiv\text{CCH}_2$), 71.73 ($\text{HC}\equiv$), 32.19 (OCOCH_2), 23.09 (COCH_2CH_2), 16.89 ($\equiv\text{CCH}_2$). HRMS (MALDI-TOF): 552.2868 [M^+ , calcd 552.2301].

1,2-bis(1,4-phenylene)-1,2-diphenylvinyl bis(11-undecynoate) [3(10)]. The synthetic procedures are similar to those of **3(5)** described above. White wax-like solid, yield 90.6%. IR (KBr), ν (cm^{-1}): 3297 ($\text{HC}\equiv$ stretching), 2116 ($\text{C}\equiv\text{C}$ stretching), 1757 ($\text{C}=\text{O}$ stretching). ^1H NMR (400 MHz, CDCl_3), δ (TMS, ppm): 7.10, 7.00, 6.83 (18H, aromatic protons), 2.50 (m, 4H, OCOCH_2), 2.18 (m, 4H, $\equiv\text{CCH}_2$), 1.93 (t, 2H, $\text{HC}\equiv$), 1.71 (m, 4H, $\text{OCOCH}_2\text{CH}_2$), 1.51 (m, 4H, $\equiv\text{CCH}_2\text{CH}_2$), 1.31 [m, 16H, $\text{OCOCH}_2\text{CH}_2(\text{CH}_2)_4$]. ^{13}C NMR (100 MHz, CDCl_3), δ (TMS, ppm): 172.06 ($\text{C}=\text{O}$), 149.21, 143.35, 141.07, 140.27, 132.24, 131.33, 127.81, 127.67, 126.55, 120.83, 120.69, 84.69 ($\equiv\text{C}-\text{CH}_2$), 68.10 ($\text{HC}\equiv$), 34.35 (OCOCH_2), 29.08, 28.99, 28.87, 28.63, 28.40, 24.83, 18.36 ($\equiv\text{CCH}_2$). HRMS (MALDI-TOF): m/e 692.5381 [M^+ , calcd 692.3866].

2.4 Click Polymerization

Polycycloaddition reactions of the diynes with the diazides were carried out under nitrogen in Schlenk tubes. Typical experimental procedures for the click polymerization of **1(5)** with **2** are given below as an example.

In a 15 mL Schlenk tube were placed 46.5 mg (0.1 mmol) of **1(5)**, 38.0 mg (0.1 mmol) of **2** and 3.7 mg of $\text{Cu}(\text{PPh}_3)_3\text{Br}$. 2 mL of DMF was then injected. After stirring at 60 °C for 12 h, the reaction mixture was diluted with 3 mL of DMF and added dropwise into 500 mL of hexane/THF mixture (20:1) through a cotton filter under stirring. The precipitates were allowed to stand overnight, collected by filtration, and dried under vacuum at 40 °C to a constant weight. A light yellow solid of **P4(5)** was obtained in 94.1% yield. M_w 11800, M_w/M_n 1.66. IR (KBr), ν (cm^{-1}): 1753 ($\text{C}=\text{O}$ stretching). ^1H NMR (400 MHz, $\text{DMSO}-d_6$), δ (TMS, ppm): 8.46 (triazole proton), 7.58, 7.08, 6.96 (aromatic protons), 4.34 (methylene protons connected to triazole ring), 2.53 (OCOCH_2), 1.84 (NCH_2CH_2), 1.63 ($\text{OCOCH}_2\text{CH}_2$), 1.29 ($\text{OCOCH}_2\text{CH}_2\text{CH}_2$). ^{13}C NMR (100 MHz, $\text{DMSO}-d_6$), δ (TMS, ppm): 171.50 ($\text{C}=\text{O}$), 149.80, 145.80, 142.84, 142.48, 140.18, 136.71, 131.08, 130.54, 128.82, 128.74, 127.71, 127.65, 127.51, 126.52, 124.42, 124.33, 122.05, 121.06 (aromatic carbons), 49.13 (NCH_2), 33.07 (OCOCH_2), 29.03 (NCH_2CH_2), 24.97 ($\text{NCH}_2\text{CH}_2\text{CH}_2$), 23.54 ($\text{OCOCH}_2\text{CH}_2$).

Characterization Data of P4(10) (Table 1, no. 10). Light yellow solid, yield 94.8%. M_w 14600, M_w/M_n 1.47. IR (KBr), ν (cm^{-1}): 1755 ($\text{C}=\text{O}$ stretching). ^1H NMR (400 MHz, CDCl_3), δ (TMS, ppm): 7.66 (triazole proton), 7.55, 7.14, 7.10 (aromatic protons), 4.77, 4.35, 2.57, 1.90, 1.76, 1.32. ^{13}C NMR (100 MHz, CDCl_3), δ (TMS, ppm): 172.31 ($\text{C}=\text{O}$), 150.18, 147.51, 143.58, 143.54, 143.44, 143.20, 143.13, 140.75, 137.99, 131.82, 131.76, 128.06, 127.85, 127.81, 126.62, 125.10, 124.96, 121.86 (aromatic carbons), 50.35, 34.38, 30.32, 29.26, 29.14, 29.02, 28.94, 26.44, 24.91.

Characterization Data of P5(5) (Table 1, no. 6). White solid, yield 97.1%. M_w 11400, M_w/M_n 1.91. IR (KBr), ν (cm^{-1}): 1755 ($\text{C}=\text{O}$ stretching). ^1H NMR (400 MHz, $\text{DMSO}-d_6$), δ (TMS, ppm): 7.88 (triazole proton), 7.65, 7.16, 7.14, 6.95, 6.86 (aromatic protons), 4.30 (NCH_2), 2.67 (methylene protons connected to triazole carbon), 2.55 (OCOCH_2), 1.91 ($\text{triazole}-\text{CH}_2\text{CH}_2\text{CH}_2$), 1.82 (NCH_2CH_2), 1.64 ($\text{biphenyl}-\text{OCOCH}_2\text{CH}_2$), 1.30 ($\text{NCH}_2\text{CH}_2\text{CH}_2$). ^{13}C NMR (100 MHz, $\text{DMSO}-d_6$), δ (TMS, ppm): 171.49, 171.10 ($\text{C}=\text{O}$), 149.83, 148.68, 148.64, 142.74, 142.68, 140.27, 140.22, 139.81, 136.74, 131.38, 130.41, 127.74, 127.66, 127.53, 126.52, 126.45, 122.08, 121.79, 121.01, 120.93 (aromatic carbons), 48.83 (NCH_2), 33.10, 32.67, 29.16, 25.07, 24.06, 23.97, 23.53.

Characterization Data of P5(10) (Table 1, no. 11). White solid, yield 87.0%. M_w 12900, M_w/M_n 1.72. IR (KBr), ν (cm^{-1}): 1757 ($\text{C}=\text{O}$ stretching). ^1H NMR (400 MHz, CDCl_3), δ (TMS, ppm): 7.53 (triazole proton), 7.30, 7.14, 7.12, 7.10, 7.00, 6.82 (aromatic protons), 4.30 (NCH_2), 2.82, 2.56, 2.10, 1.88, 1.76, 1.40, 1.31. ^{13}C NMR (100 MHz, CDCl_3), δ (TMS, ppm): 172.27, 171.56 ($\text{C}=\text{O}$), 150.17, 149.12, 149.05, 143.28, 143.19, 141.01, 140.91, 140.26, 137.98, 132.20, 131.27, 128.05, 127.79, 127.66, 126.64, 126.55, 121.85, 120.75, 120.62 (aromatic carbons), 50.18 (NCH_2), 34.35, 33.55, 30.27, 29.25, 29.13, 29.01, 28.92, 26.45, 24.86, 24.81, 24.52.

Characterization Data of P6(5) (Table 1, no. 7). White solid, yield 75.2%. M_w 16200, M_w/M_n 2.0. IR (KBr), ν (cm^{-1}): 1755 ($\text{C}=\text{O}$ stretching). ^1H NMR (400 MHz, $\text{DMSO}-d_6$), δ (TMS, ppm): 7.82 (triazole proton), 7.64, 7.09, 6.94, 6.84 (aromatic protons), 4.28 (NCH_2), 2.54, 1.82, 1.63, 1.54, 1.24. ^{13}C NMR (100 MHz, $\text{DMSO}-d_6$), δ (TMS, ppm): 172.68, 171.50 ($\text{C}=\text{O}$), 149.83, 148.70, 142.72, 140.19, 139.81, 136.72, 131.40, 130.41, 127.66, 127.50, 126.68, 126.48, 122.06,

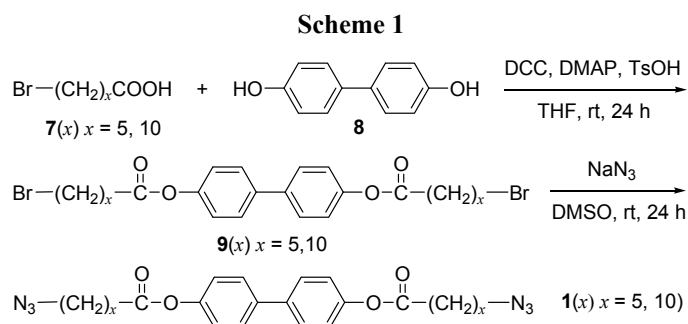
120.91 (aromatic carbons), 48.79 (NCH₂), 33.27, 33.12, 29.16, 28.73, 28.40, 28.33, 28.15, 25.06, 24.87, 24.25, 24.09, 23.54.

Characterization Data of P6(10) (Table 1, no. 13). White solid, yield 63.6%. *M_w* 11900, *M_w/M_n* 1.61. IR (KBr), ν (cm⁻¹): 1757 (C=O stretching). ¹H NMR (400 MHz, CDCl₃), δ (TMS, ppm): 7.53 (triazole proton), 7.24, 7.15, 7.12, 7.08, 7.02, 6.82 (aromatic protons), 4.29 (NCH₂), 2.69, 2.57, 2.48, 1.87, 1.76, 1.69, 1.33, 1.31. ¹³C NMR (100 MHz, CDCl₃), δ (TMS, ppm): 171.67, 171.41 (C=O), 149.58, 148.61, 148.54, 142.74, 142.63, 140.34, 140.24, 139.65, 137.39, 131.59, 130.69, 127.45, 127.18, 127.05, 126.01, 125.92, 121.25, 120.20, 120.06 (aromatic carbons), 49.51 (NCH₂), 33.75, 33.73, 29.71, 28.82, 28.67, 28.54, 28.52, 28.42, 28.40, 28.34, 25.87, 25.05, 24.27, 24.21.

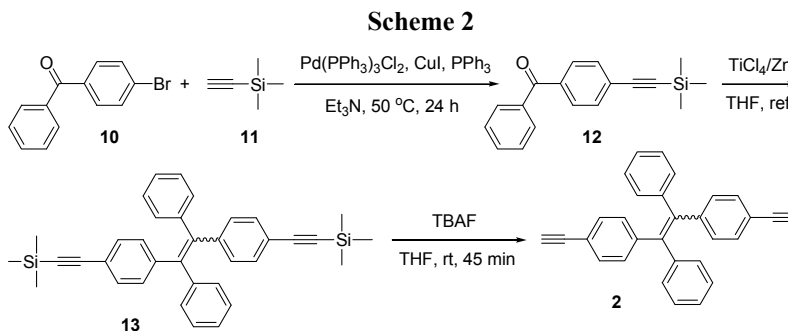
3. RESULTS AND DISCUSSION

3.1 Monomer Synthesis

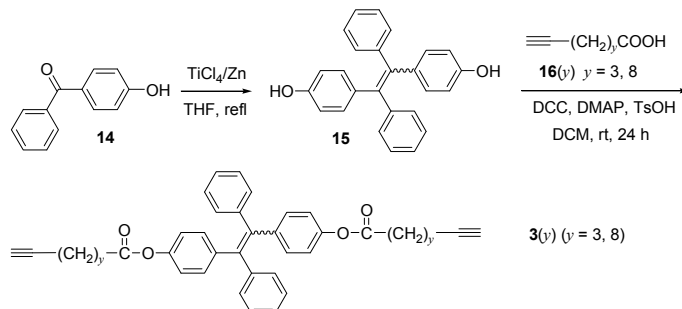
With a view to synthesize AIE-active liquid crystalline polymers by click reaction, we prepared biphenyl-containing diazides with different aliphatic spacer lengths according to Scheme 1. We first esterified 4,4'-biphenol (**8**), with ω -bromoalkanoic acid **7(x)** in the presence of DCC, DMAP, and TsOH. The resulting compounds **9(x)**, were then reacted with sodium azide, furnishing the desirable products **1(x)**.



We also synthesized TPE-functionalized diynes **2** and **3(y)**, according to the synthetic routes shown in Scheme 2 and 3. To obtain compound **2**, we first prepared compound **12** by palladium-catalyzed cross-coupling of 4-bromobenzophenone (**10**) with trimethylsilylacetylene (**11**). McMurry coupling of **12** catalyzed by TiCl₄ and Zn afforded **13**, which converted into **2** by cleavage of its trimethylsilyl groups in basic medium. Diynes **3(y)** are structural congeners of **2** but their triple bond functionalities are connected to the TPE core through alkyl chains and ester groups. They were synthesized by McMurry coupling of 4-hydroxybenzophenone (**14**) followed by esterification with β -alkynoic acids **16(y)**. All the reactions proceeded smoothly and the desirable monomers were obtained in high yields. The monomers were characterized by standard spectroscopic methods, from which satisfactory analysis data corresponding to their molecular structures were obtained (see Experimental Section for details).



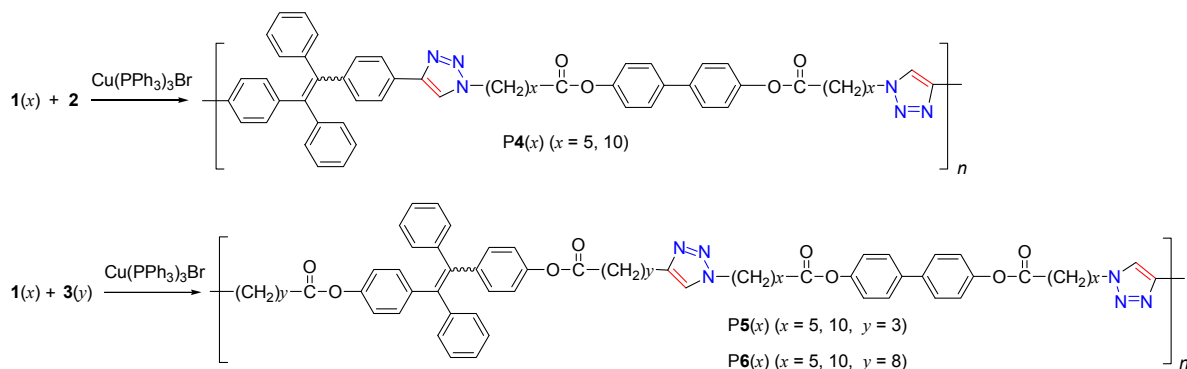
Scheme 3



3.2 Click Polymerization

We then carried out the polycycloaddition reactions of **1(x)** with **2** and **3(y)** according to Scheme 4. We first tried to polymerize **1(5)** and **2** by $\text{Cu}(\text{PPh}_3)_3\text{Br}$, an effective organosoluble catalyst for the 1,4-regioregular 1,3-dipolar cycloaddition.^{29,31} Reaction conducted in THF at 60 °C for 12 h gives some THF-insoluble products, which can dissolve readily in DMF. After precipitation of the solution into hexane/THF mixture, **P4(5)** is isolated in a yield of 85.1% (Table 1, no. 1). The M_w and M_w/M_n of its THF soluble fraction are 11 800 and 1.44, respectively. The mixture remains homogenous throughout the polymerization process when the polymerization is carried out in DMF. Although a higher yield is obtained, the polymer is soluble only in DMF and DMSO but dissolves partially in THF, DCM, and chloroform. The limited solubility of the polymer should be ascribed to the rigidity of the polymer chain and its higher molecular weight. We thus fine tuned the molecular weight of the polymer by lowering the reaction time to 6 h and obtained completely soluble products albeit in a low yield. In our previous study, we found that ruthenium catalysts can produce polymers with better solubility due to the formation of more twisted 1,5-triazole units.³³ When we used $\text{Cp}^*\text{Ru}(\text{PPh}_3)_2\text{Cl}$ as catalyst for the polymerization of **1(5)** and **2**, a soluble polymer is isolated in a high yield but its molecular weight is rather low.

Scheme 4



The polymerizations of other monomer pairs are conducted using $\text{Cu}(\text{PPh}_3)_3\text{Br}$ as catalyst in THF or DMF. As depicted in Table 1, nos. 5–14, all the polymers are obtained in high yields (63.6–94.8%) with moderate M_w values of 8 900–16 200. Generally, the polymerizations performed in DMF give much higher yields than those conducted in THF. Thanks to their long alkyl chains, **P5(x)** and **P6(x)** possess good solubilities in THF, DCM, and chloroform.

Table 1. Click Polymerizations of Diazides with Diynes^a

no.	solvent	time (h)	yield (%)	M_w^b	M_w/M_n^b
1(5) + 2					
1	THF	12	85.1	11 800 ^c	1.42
2	DMF	12	94.1	11 800 ^c	1.66
3	THF	6	40.0	3 400	1.30
4 ^d	THF	12	94.0	4 900	1.61
1(5) + 3(3)					
5	THF	12	63.7	8 900	1.67
6	DMF	12	97.1	11 400	1.91
1(5) + 3(8)					
7	THF	12	75.2	16 200	2.00
8	DMF	12	79.3	10 200	1.77
1(10) + 2					
9	THF	12	94.5	14 800	1.48
10	DMF	12	94.8	14 600	1.47
1(10) + 3(3)					
11	THF	12	87.0	12 900	1.72
12	DMF	12	90.4	12 900	1.76
1(10) + 3(8)					
13	THF	12	63.6	11 900	1.61
14	DMF	12	85.4	12 900	1.62

^a Carried out at 60 °C under nitrogen using Cu(PPh₃)₃Br as catalyst unless otherwise specified. ^b Estimated by GPC in THF on the basis of a polystyrene calibration. ^c THF soluble fraction. ^d Cp^{*}Ru(PPh₃)₂Cl was used as catalyst.

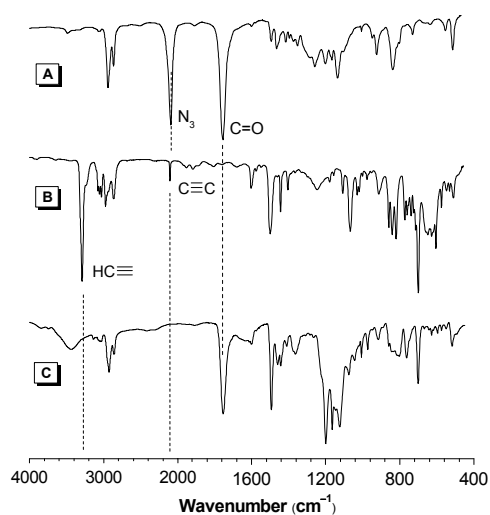


Figure 1. IR spectra of (A) monomer 1(5), (B) monomer 2, and (C) their polymer P4(5) (sample taken from Table 1, no. 2).

3.3 Structural Characterization

All the polymers are characterized by spectroscopic techniques and give satisfactory analysis data corresponding to their expected structures. An example of the IR spectrum of P4(5) is shown in Figure 1. The spectra of its monomers **1**(5) and **2** are also given in the same figure for comparison. Monomer **1**(5) shows absorption band at 2906 cm^{-1} due to the stretching vibration of its azido functionality. The $\text{HC}\equiv$ and $\text{C}\equiv\text{C}$ stretching vibrations of monomer **2** are observed at 3276 and 2107 cm^{-1} . After polymerization, all these are absent in the spectrum of P4(5), indicating that all the azido groups of **1**(5) and triple bonds of **2** have been consumed by polycycloaddition.

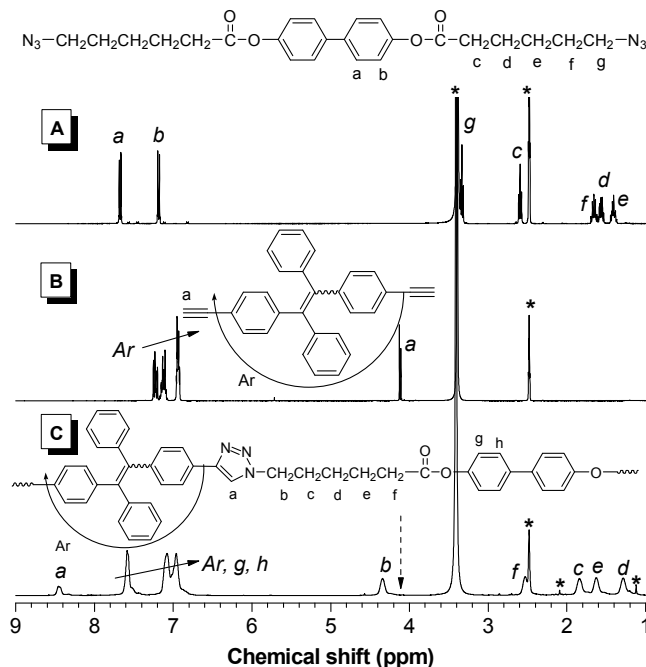


Figure 2. ^1H NMR spectra of (A) monomer **1**(5), (B) monomer **2**, and (C) their polymer P4(5) (sample taken from Table 1, no. 2) in $\text{DMSO}-d_6$ at room temperature. The solvent peaks are marked with asterisks.

We further characterized the polymers by NMR spectroscopy. Figure 2 shows the ^1H NMR spectra of monomers **1**(5) and **2**, and their corresponding polymer P4(5) in $\text{DMSO}-d_6$. The polymer gives no peaks corresponding adjacent to the azido group of **1**(5) and acetylenic proton of **2** at $\delta \sim 4.1$ and ~ 3.3 , respectively (Figures 2A and 2B). Meanwhile, new resonances assigned to the absorptions of the olefin proton of 1,4-disubstituted triazole ring and its neighboring methylene protons are emerged at $\delta \sim 8.5$ and $\delta \sim 4.3$. No olefin proton resonance associated with 1,5-disubstituted is detected and all the peaks can be readily assigned, suggesting that the polymeric product is indeed P4(5) with molecular structure as shown in Figure 2C.

Figure 3 shows the ^{13}C NMR spectrum of polymer P4(5) along with those of monomer **1**(5) and **2**. While the methylene carbon next to the azido group of **1**(5) resonate at $\delta 50.31$ (Figure 3A), the absorptions of the acetylenic carbon atoms of **2** occur at $\delta 83.14$ and 80.88 (Figure 3B). The spectrum of P4(5) shows no these absorptions but new peaks associated with the resonances of the olefin carbons at $\delta 145.81$ and 142.76 . This result testifies that the azido groups of **1**(5) and triple bonds of **2** have been cyclized into triazole rings in P4(5), which well agrees with those from the IR and ^1H NMR analyses.

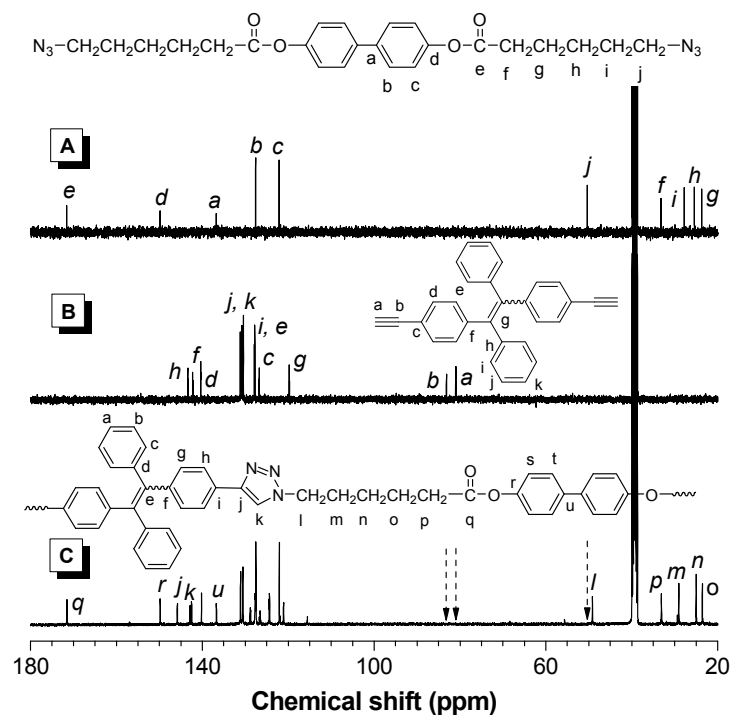


Figure 3. ^{13}C NMR spectra of (A) monomer 1(5), (B) monomer 2, and (C) their polymer P4(5) (sample taken from Table 1, no. 2) in $\text{DMSO}-d_6$ at room temperature.

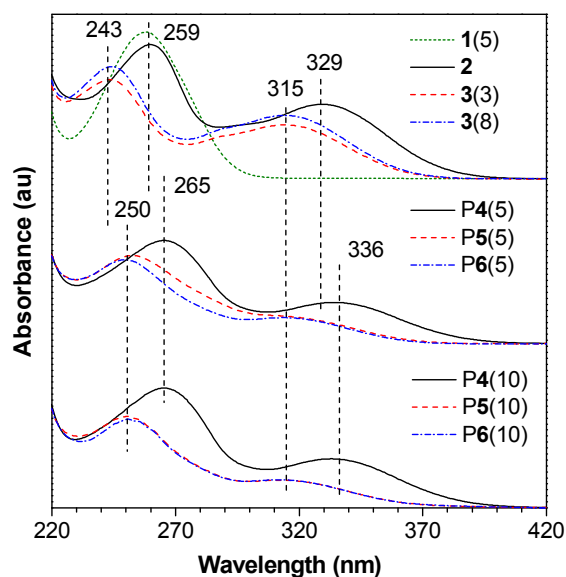


Figure 4. Absorption spectra of monomers and polymers in THF. Concentration: 2×10^{-5} M (monomers), 0.008 mg/mL (polymers). Soluble fraction of P4(5) in THF was used for the measurement.

3.4 Electronic Transitions

Figure 4 shows the absorption spectra of the monomers and polymers in THF. The biphenyl pendant of 1(5) absorbs at 257 nm, while the absorption of the TPE moiety of monomer 2 occurs at 259 and 329 nm. After polymerization, their corresponding polymer P4(5) absorbs at slightly longer wavelengths of ~265 and 336 nm. Clearly, the polymer is more

conjugated because of electronic communication between the TPE unit and the newly formed triazole ring. Due to the structural similarity, polymer P4(10) shows an absorption profile identical to that of P4(5). The UV spectra of P5(x) and P6(x) are similar, featuring two maximum at 250 and 315 nm. Their spectra patterns are resembled to those of 3(y) because their triazole rings are well separated from the TPE units by long alkyl spacers, which have hampered their electronic interactions.

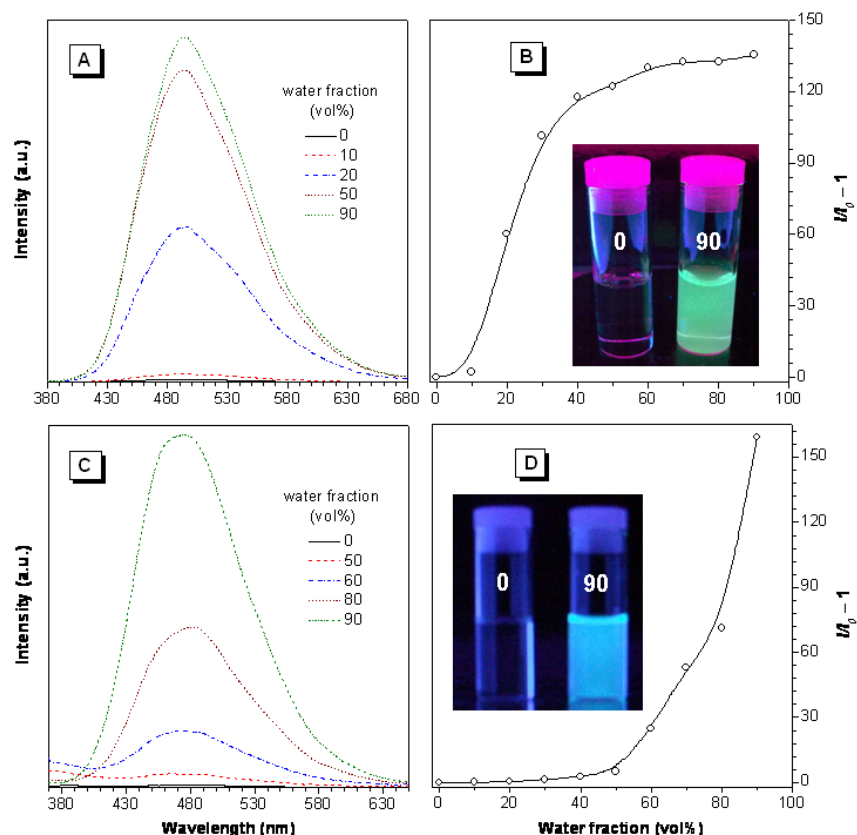


Figure 5. Emission spectra of (A) P4(5) in DMF/H₂O and (C) P6(5) in THF/H₂O mixtures with varied water fractions. Plots of $(I/I_0 - 1)$ values versus water fractions of the aqueous mixtures at (B) 493 and (D) 475 nm for P4(5) and P6(5), respectively. Photos of P4(5) and P6(5) in DMF and THF with 0 and 90% water contents taken under UV light, respectively, are given in panels B and D. Concentration (mg/mL): 0.044 [P4(5)], 0.06 [P6(5)], excitation wavelength (nm): 350 [P4(5)], 340 [P6(5)].

3.5 Aggregation Induced Emission

TPE is a well-known AIE luminogen and it is thus anticipated that our TPE-containing polymers are also AIE-active. To confirm this, we investigate their emission behaviors in solvent/nonsolvent mixtures. As shown in Figure 5A, polymer P4(5) is almost nonluminescent in pure DMF. Addition of water into its THF solution, has, however, enhanced its light emission. The higher the water content, the stronger is the light emission. In 90% aqueous mixture, the emission intensity is >135-fold higher than that in the pure DMF solution, exhibiting a bright emission with its maximum at 493 nm (Figure 5B). Since biphenyl emits in the UV region, the visible emission of P4(5) should be, in most cases, originated from its TPE chromophoric units. The photographs depicted in the inset exemplify the nonemissive and strongly luminescent nature of the DMF solution and 90% aqueous mixtures. Clearly, the AIE characteristics of the TPE units are preserved when they are incorporated into polymer. Polymer P6(5) also exhibits typical AIE behavior. As can be seen in Figures 5C and 5D, the polymer emits no light in THF but gives a strong sky-blue emission at 475 nm when aggregated in the aqueous mixture. The emission is gradually intensified with increasing water content in the THF/water mixture. At 90% water content, the intensity is more than 159-fold higher than that in pure THF solution. Similar phenomenon are also

observed in P5(x) and P6(10). In their 90% aqueous mixtures, the emission intensities are > 150-fold higher than those in pure THF.

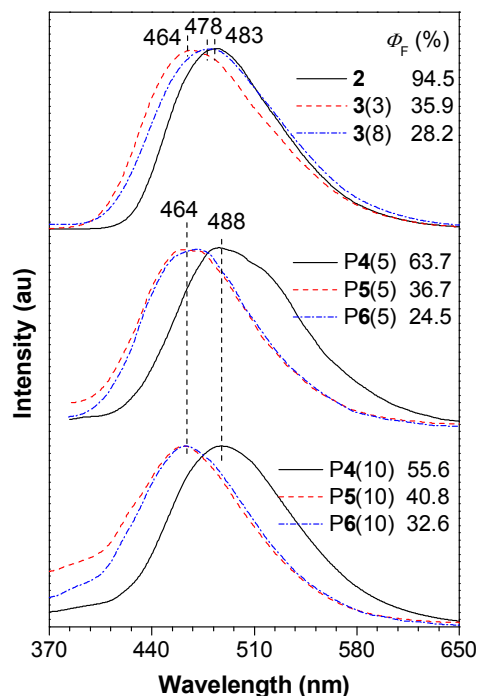


Figure 6. Emission spectra of thin films of monomers **2**, **3(3)**, **3(8)**, and polymers **P4(x)**, **P5(x)**, and **P6(x)** at room temperature. Excitation wavelength: 350 nm. Quantum yields of the polymers in THF: 0.67% [**P4(5)**, THF-soluble fraction], 0.51% [**P5(5)**], 0.28% [**P6(5)**], 0.19% [**P4(10)**], 0.20% [**P5(10)**], 0.26% [**P6(10)**].

We also investigated their photophysical properties in the solid state. Thanks to the AIE effects of the TPE units, the bulk solids of the **P4(x)**, **P5(x)**, and **P6(x)** are highly emissive under UV light illumination. The solid films of the polymers are also capable of emitting light intensely. Figure 6 depicts their emission spectra, for comparison, the spectra of their monomers **2** and **3(y)** are also given in the same figure. Since **P4(5)** and **P4(10)** possess higher conjugation, they emit at slightly longer wavelengths (~488 nm) than **2** (483 nm). The emission maxima of **P5(x)** are located at wavelengths similar to that of **3(3)**. Those of **P6(x)** are, however, blue-shifted from **3(8)** by 14 nm. The relative longer alkyl spacers in **P6(x)** may have effectively hampered the interactions between the TPE units, thus resulted in emission at the bluer region.

To have a quantitative comparison, the quantum yields (Φ_F 's) of the polymers in THF solutions and solid film states are measured. The Φ_F values in solutions are quite low. Those of their solid films are, however, much higher and ranged from 24.5 to 63.7%. Closer inspection reveals that Φ_F values of the monomers and polymers are varied by the spacer length. For example, when the methylene unit is progressively increased from **P4(5)** to **P5(5)** and then **P6(5)**, the quantum yield decreases from 63.7% to finally 24.5%. Thus, the incorporation of electronically saturated alkyl chains in the monomers and polymers are harmful to their light emissions, presumably due to the obstruction of the TPE aggregation formation.

3.6 Thermal Stability

Since the formation of mesophases of thermotropic liquid crystals is realized by the application of heat, the thermal stability of the polymers is thus of primary concern. Figure 7 gives the TGA thermograms of the polymers recorded under nitrogen. All the polymers show high resistance to thermolysis, with 5% weight loss (T_d) occurring from 346 to 406 °C. The T_d values are much higher than that of polystyrene (330 °C), a stable commodity polymer.³⁴ The high thermal stability of the polymers renders them useful for practical applications.

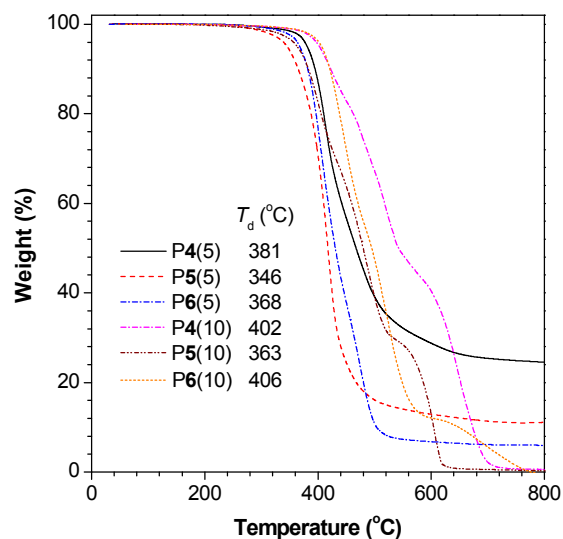


Figure 7. TGA thermograms of P4(x), P5(x), and P6(x) measured under nitrogen at a heating rate of 20 °C/min.

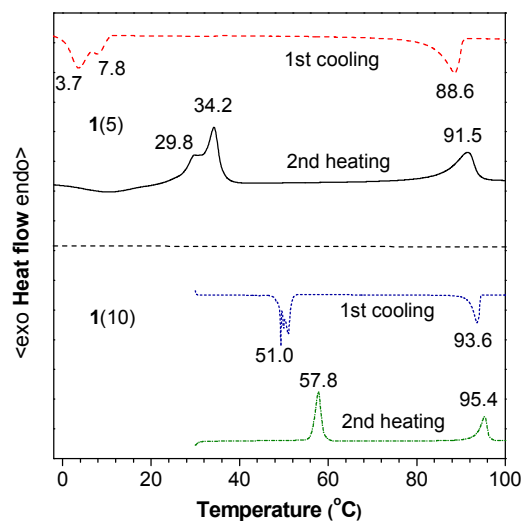


Figure 8. DSC thermograms of monomers 1(5) and 1(10) recorded under nitrogen during the first cooling and second heating cycles with a scan rate of 10 °C/min.

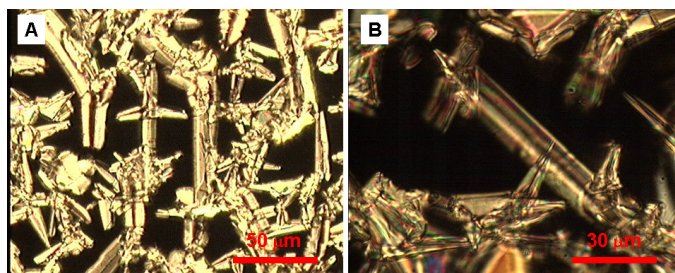


Figure 9. Mesomorphic textures observed on cooling (A) 1(5) to 92.8 °C and (B) 1(10) to 95.4 °C from their isotropic states at a cooling rate of 0.5 and 0.2 °C/min, respectively.

3.7 Mesomorphism

After checking the thermal stability of the polymers, we investigated their mesomorphic properties. Since monomers **1**(5) and **1**(10) contain mesogenic biphenyl unit, we thus first checked whether they are liquid crystalline. Figure 8 shows the DSC thermograms of **1**(5) and **1**(10) recorded during the first cooling and second heating processes, while their POM textures observed on cooling from their isotropic liquids are given in Figure 9.

During the first cooling cycle, **1**(5) shows three exothermic peaks at 88.6, 7.8, and 3.7 °C. POM observation reveals that upon cooling **1**(5) from the isotropic state (i) to 94.2 °C, mosaic texture of smectic B phase (S_B) with lancet³⁵ emerges from the homotropic dark background. More anisotropic domains appear at 92.8 °C and their sizes grow bigger when the temperature is further lowered (Figure 9A). The transition peaks at 7.8 and 3.7 °C are ascribed to S_B -crystal (k) and k-k transitions, respectively. The DSC curve recorded in the second heating cycle is the mirror image of that obtained in the first cooling scan, three endothermic peaks corresponding to the k-k, k- S_B , and S_B -i transitions are detected at 29.8, 34.2 and 91.5 °C, respectively.

Monomer **1**(10) is the congener of **1**(5) with much longer flexible spacers and it is of interest to study how it behaves mesomorphically. As depicted in Figure 8, during the first cooling cycle, **1**(10) shows two distinct transition peaks at 51.0 and 93.6 °C. When it is cooled from its isotropic state to 95.4 °C, mosaic texture of S_B mesophase with lancet similar to that of **1**(5) is observed. The second heating scan detects two endothermic peaks at 57.8 and 95.4 °C, which are associated to the k- S_B and S_B -i transitions, respectively.

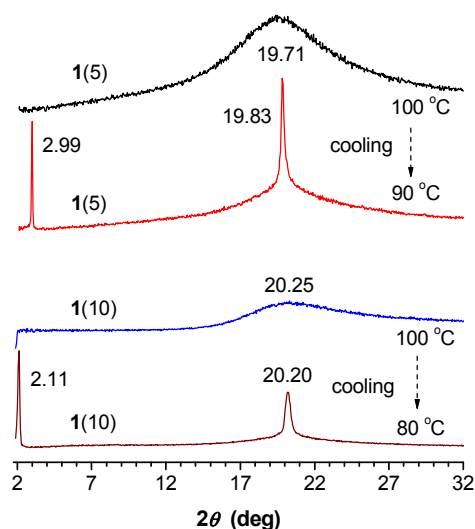


Figure 10. X-ray diffraction patterns of **1**(5) and **1**(10) obtained on cooling from their isotropic liquids.

To obtain more information on the packing arrangements in the mesophases of the monomers, we carried out the 1D-WAXD measurements. The diffractograms of **1**(5) and **1**(10) obtained at 100 °C display only diffuse halos at high angle, indicative of their isotropic feature (Figure 10). When **1**(5) is cooled to 90 °C, two sharp peaks at $2\theta = 2.99$ and 19.83° are recorded. The d -spacing calculated from the first peak is 29.53 Å and is comparable molecular length of **1**(5) ($l = 31.63$ Å) in its fully extended conformation. The peak at $2\theta = 19.83^\circ$ has a narrow full width at half maximum of 0.326° . This suggests the molecules are orderly aligned within the same layer, which is the characteristic of S_B mesomorphic phase.

Similar WAXD pattern is observed in **1**(10) when it is cooled to 80 °C. The reflection at $2\theta = 20.20^\circ$ gives the average distance of the shorter preferred spacing ($d = 4.39$ Å) occurring in the lateral packing arrangement of the mesogenic pendants. The layer spacing derived from the peak at 2.11° is 41.84 Å, which well approaches to the molecular length of **1**(10) ($l = 44.07$ Å) at its most extended conformation. All these features confirm the formation of S_B phase.

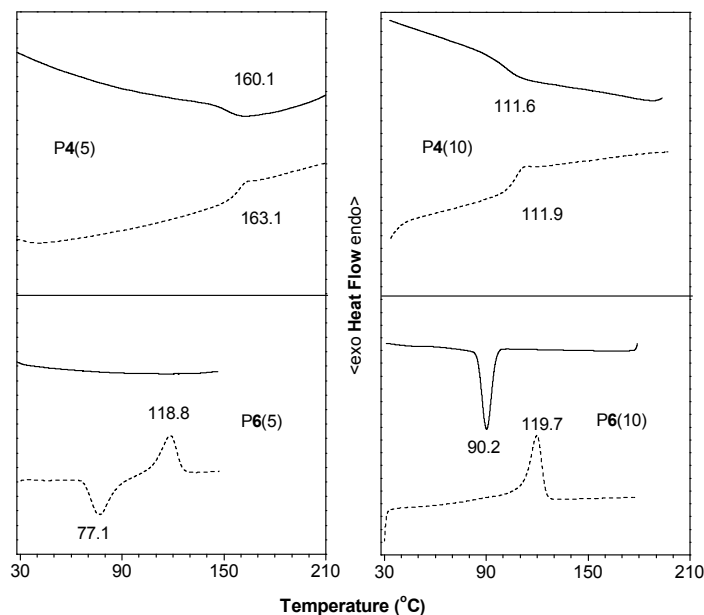


Figure 11. DSC thermograms of the polymers recorded under nitrogen during the first cooling (solid line) and second heating (dash line) cycles at a scan rate of 10 °C /min.

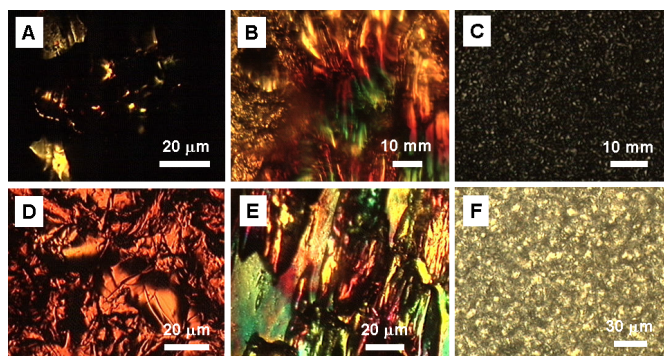


Figure 12. Mesomorphic textures observed on cooling (A) P4(5) to 159.9 °C, (B) P5(5) to 89.9 °C, (C) P6(5) to 94.9 °C, (D) P4(10) to 250.6 °C, (E) P5(10) to 69.8 °C, and (F) P6(10) to 114.9 °C from their melting states at a cooling rate of 1 °C/min. Photos in (A), (B), (D), and (E) are taken after application of a shearing force.

We then continued our study on the mesomorphic properties of the polymers. We first checked the thermal transitions of the polymers by DSC. In the first cooling cycle, P4(5), P4(10), and P6(10) exhibit exothermic peaks at 160.1, 111.6, and 90.2 °C (Figure 11), respectively, associated with the transition from the isotropic liquid to liquid crystalline phase. The corresponding LC-i transitions are observed at 163.1, 119.6, and 119.7 °C in the second heating scan. The thermogram of P6(5) recorded in the first cooling cycle is basically a flat line parallel to the abscissa. On the contrary, two peaks related to chain rearrangement and LC-i transition are observed at 77.1 and 118.8 °C, respectively.

No birefringences are observed when P4(5), P4(10), P5(5) and P5(10) are cooled from their melted states. Anisotropic domains are, however, emerged under shearing (Figures 12A, B, D, and E). Thus, all the polymers are mesomorphic. The liquid crystalline domains of the polymers are too small to be observed without external stimuli. Such phenomenon should be caused by the high rigidity of the main chain, which impedes the packing arrangements of the mesogenic units. When a shear force is applied, many domains merge together and aligned along the shear direction, thus them observable under POM.

Thanks to the relative longer flexible spacers in P6(5) and P6(10) which render the mesogenic units more freedom to pack, small entities are emerged from the homotropic dark background when their isotropic liquids are cooled. The entities grow bigger upon cooling but their development into a typical texture seems to be a difficult task. We attempted to grow such the crystals with care but failed to obtain any characteristic texture.

We carried out 1D-WAXD experiments of the polymers at different temperatures in order to gain more information concerning their molecular arrangements, and modes of packing in the mesophases. As shown in Figure 13A, the diffractogram of thin film of P4(10) casted from its THF solution at 40 °C shows a broad peak at $2\theta = 6.27^\circ$ and a halo 18.91°. The spectral profile keeps almost unchanged when the polymers is heated to temperatures up to 210 °C. The diffractogram also changes little upon cooling (Figure 13B). It indicates that the film formed from the solution is liquid crystalline and the mesophase is stable during both heating and cooling processes. This result is quite similar to those observed in Zhou's mesogen-jacketed mesomorphic polymers, in which the liquid-crystalline phases are stable at both elevated and low temperatures.³⁶ It is in some sense understandable when we take the high stiffness of the polymer main chain into consideration. The rigid polymer strand hampers the packing of the mesogenic units but on the other hand, stabilizes and fixes their alignment. The d -spacing associated with the diffuse halo changes at high temperatures, which is commonly observed in LCs exhibiting nematicity.³⁷ According to its poor packing feature and temperature-dependent d -spacing phenomenon, we can assign the mesomorphic phase of P4(10) to be nematic.

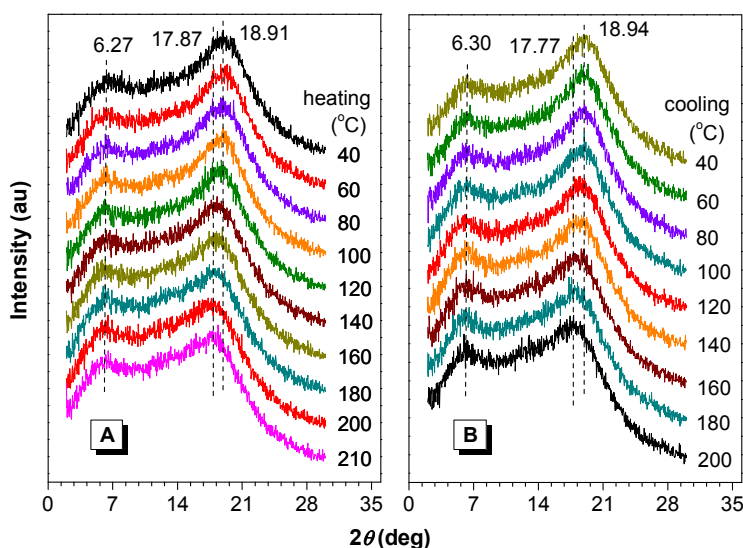


Figure 13. X-ray diffractograms of P4(10) at different temperatures obtained during the (A) heating and (B) cooling cycles.

When three more methylene units are introduced into P4(10), the resultant polymer P5(10) shows better mesogenic packing. Its X-ray diffractograms measured at different temperatures during the heating and cooling cycles are depicted in Figure 14. At 40 °C, the diffractogram shows a reflection peak and two halos at $2\theta = 3.93^\circ$, 8.30° and 20.48° , from which d -spacings of 22.46, 10.64, and 4.32 Å are derived, respectively (Figure 14A). The appearance of these featured peaks suggests the formation of smatic mesophase. The peak at 3.93° becomes weaker at 90 °C and disappears completely at 110 °C. In the subsequent cooling process from 150 to 40 °C, no observable change is observed in the diffractograms. This indicates that the mesogenic packing lost in the heating scan cannot be recovered by subsequent cooling process due to the low chain mobility caused by the still rigid polymer strand.

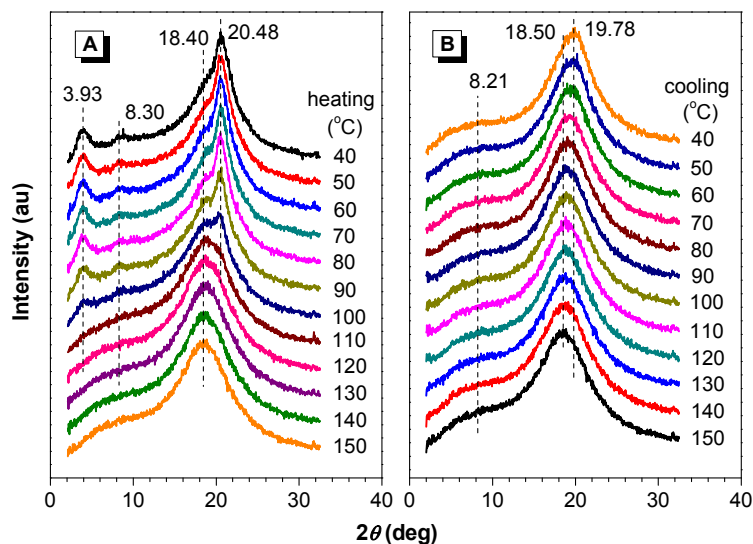


Figure 14. X-ray diffractograms of P5(10) at different temperatures obtained during the (A) heating and (B) cooling cycles.

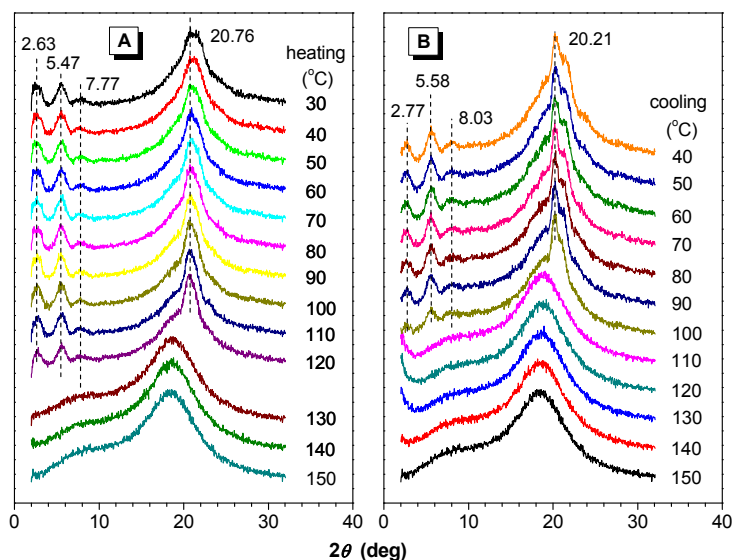


Figure 15. X-ray diffractograms of P6(10) at different temperatures obtained during the heating and cooling cycles.

Polymer P6(10) has even longer flexible spacers than that of P5(10), and its temperature-variable WAXD diagrams are shown in Figure 15. At 30 °C, three peaks and one diffuse halo at $2\theta = 2.63, 5.47, 7.77,$ and 20.76° are observed. When the sample is heated to 130 °C, the former three reflections disappear, revealing that the isotropic state is reached and the mesogens are now randomly orientated. These peaks, are, however, emerged again upon cooling (Figure 15B), thanks to the relative more flexible chain of P6(10), which provides little constraint for the mesogens to pack in the mesophase. From the XRD profile, it is reasonable to assign its mesogenic phase as smatic. For detailed phase identification, further investigation on its molecular packing is required and is actively undergone in our laboratory. Other WAXD measurement for P4(5), P5(5), and P6(5) are also conducted (not given here). No obvious signals at low angles are recorded, suggesting that all the polymers exhibit nematicity at high temperature.

4. CONCLUSIONS

In this paper, regioselective 1,3-dipolar polycycloadditions of biphenyl-containing diazides and tetraphenylethene-carrying diynes are initiated by $\text{Cu}(\text{PPh}_3)_3\text{Br}$ in THF or DMF generating soluble polytriazoles in high yields (up to 94.8%) narrow molecular weight distributions.

All the polymers are AIE-active. While they emit weakly in solutions with Φ_F values not more than 0.67%, they become strong emitters in the aggregated states with Φ_F values up to 63.7%. The Φ_F value is sensitive to the spacer length and decreases when the ethylene unit in the polymers becomes higher.

All the polymers enjoy high thermal stability and are liquid crystalline at high temperatures. While polymers **P4**(*x*) possess rigid main chains and thus exhibit nematicity, their counterparts with longer spacer lengths, i.e. **P5**(*x*) and **P6**(*x*), show better mesogenic packing and form smectic phases at high temperatures. Our results have shown that through rational design, it is feasible to create liquid crystals with strong light emissions. We are currently working on the synthesis of new mesomorphic polymers and studied their polarized emission. Details will be published in a separate paper.

5. ACKNOWLEDGEMENTS

This work was partially supported by the Hong Kong Research Grants Council (603509, 601608, and 603008), The National Science Foundation of China (20974028 and 20634020), and the Ministry of Science & Technology (2009CB623605). B.Z.T. thanks the support from the Cao Guangbiao Foundation of Zhejiang University.

REFERENCES

- [1] Gray, G. W., Ed., "Thermotropic liquid crystals," Wiley, Chichester (1987).
- [2] Kato, T., Mizoshita, N. and Kishimoto, K., "Functional liquid-crystalline assemblies: Self-organized soft materials Functional liquid-crystalline assemblies: Self-organized soft materials," *Angew. Chem. Int. Ed.* 45(1), 38-68 (2006).
- [3] Weder, C., Sarwa, C., Montali, A., Bastiaansen, C. and Smith, P., "Incorporation of photoluminescent polarizers into liquid crystal displays," *Science* 279(5352), 835-837 (1998).
- [4] Moreira, M. F., Carvalho, I. C. S., Cao, W., Bailey, C., Taheri, B. and Palffy-Muhoray, P., "Cholesteric liquid-crystal laser as an optic fiber-based temperature sensor," *Appl. Phys. Lett.* 85(12), 2691-2693 (2004).
- [5] Yablonskii, S. V., Nakano, K., Mikhailov, A. S., Ozaki, M. and Yoshino, K., "Pressure sensor based on freely suspended ferroelectric liquid crystal film," *Appl. Phys. Lett.* 80(4), 571-573 (2002).
- [6] Schadt, M., "Linear and nonlinear liquid-crystal materials, electrooptical effects and surface interactions-their application in present and future devices," *Liq. Cryst.* 14(1), 73-104 (1993).
- [7] Shimizu, Y., Monobe, H., Heinrich, B., Guillon, D., Oikawa, K. and Nakayama, K., "Mesophase semiconductors: the alignment control and self-assembling nature for transistor applications," *Mol. Cryst. Liq. Cryst.* 509, 948-954 (2009).
- [8] Sun, Q., Park, K. and Dai, L., "Liquid crystalline polymers for efficient bilayer-bulk-heterojunction solar cells," *J. Phys. Chem. C* 113(18), 7892-7897 (2009).
- [9] Lüssem, G. and Wendorff, J. H., "Liquid crystalline materials for light-emitting diodes," *Polym. Adv. Technol.* 9(7), 443-460 (1998).
- [10] Adam, D., Schuhmacher, P., Simmerer, J., Häussling, L., Siemensmeyer, K., Eitzbach, K. H., Ringsdorf, H. and Haarer, D., "Fast photoconduction in the highly ordered columnar phase of a discotic liquid-crystal," *Nature* 371(6493), 141-143 (1994).
- [11] Yoshio, M., Mukai, T., Ohno, H. and Kato, T., "One-dimensional ion transport in self-organized columnar ionic liquids," *J. Am. Chem. Soc.* 126(4), 994-995 (2004).
- [12] Zhou, M., Kidd, T. J., Noble, R. D. and Gin, D. L., "Supported lyotropic liquid-crystal polymer membranes: Promising materials for molecular-size-selective aqueous nanofiltration," *Adv. Mater.* 17(15), 1850-1853 (2005).
- [13] Yasuda, T., Ooi, H., Morita, J., Akama, Y., Minoura, K., Funahashi, M., Shimomura, T. and Kato, T., " π -Conjugated oligothiophene-based polycatenar liquid crystals: self-organization and photoconductive, luminescent, and redox properties," *Adv. Funct. Mater.* 19(3), 411-419 (2009).

- [14] Camerel, F., Bonardi, L., Schmutz, M. and Ziessel, R., "Highly luminescent gels and mesogens based on elaborated borondipyrromethenes," *J. Am. Chem. Soc.* 128(14), 4548-4549 (2006).
- [15] Seo, J., Kim, S., Gihm, S. H., Park, C. R. and Park, S. Y., "Highly fluorescent columnar liquid crystals with elliptical molecular shape: oblique molecular stacking and excited-state intramolecular proton-transfer fluorescence," *J. Mater. Chem.* 17(48), 5052-5057 (2007).
- [16] Christ, T., Glusen, B., Greiner, A., Kettner, A., Sander, R., Stumpflen, V., Tsukruk, V. and Wendorff, J. H., "Columnar discotics for light emitting diodes," *Adv. Mater.* 9(1), 48-52 (1997).
- [17] Grell, M. and Bradley, D. D. C., "Polarized luminescence from oriented molecular materials," *Adv. Mater.*, 11(11), 895-905 (1999).
- [18] Chen, S. H., Shi, H., Conger, B. M., Mastrangelo, J. C. and Tsutsui, T., "Novel vitrifiable liquid crystals as optical materials," *Adv. Mater.* 8(12), 998-1001 (1996).
- [19] Birks, J. B., "Photophysics of aromatic molecules," Wiley, London (1970).
- [20] Ting, C-H., Chen, J-T. and Hsu, C-S., "Synthesis and thermal and photoluminescence properties of liquid crystalline polyacetylenes containing 4-alkanyloxyphenyl trans-4-alkylcyclohexanoate side groups," *Macromolecules* 35(4), 1180-1189 (2002).
- [21] Jenekhe, S. A. and Osaheni, J. A. "Excimers and exciplexes of conjugated polymers," *Science* 265(5173), 765-768 (1994).
- [22] Liu, J., Lam, J. W. Y. and Tang, B. Z., "Acetylenic Polymers: Syntheses, Structures, and Functions," *Chem. Rev.* 109(11), 5799-5867 (2009).
- [23] Lam, J. W. Y., Luo, J., Dong, Y., Cheuk, K. K. L. and Tang, B. Z., "Functional polyacetylenes: synthesis, thermal stability, liquid crystallinity, and light emission of polypropiolates" *Macromolecules* 35(22), 8288-8299 (2002).
- [24] Yuan, W. Z., Lam, J. W. Y., Shen, X. Y., Sun, J. Z., Mahtab, F., Zheng, Q. and Tang, B. Z., "Functional polyacetylenes carrying mesogenic and polynuclear aromatic pendants: polymer synthesis, hybridization with carbon nanotubes, liquid crystallinity, light emission, and electrical conductivity," *Macromolecules*, 42(7), 2523-2531 (2009).
- [25] Luo, J., Xie, Z., Lam, J. W. Y., Cheng, L., Chen, H., Qiu, C., Kwok, H. S., Zhan, X., Liu, Y., Zhu, D. and Tang, B. Z., "Aggregation-induced emission of 1-methyl-1,2,3,4,5-pentaphenylsilole," *Chem. Commun.* (18), 1740-1741 (2001).
- [26] Hong, Y., Lam, J. W. Y. and Tang, B. Z., "Aggregation-induced emission: phenomenon, mechanism and applications," *Chem. Commun.* (29), 4332-4353 (2009).
- [27] Tong, H., Hong, Y., Dong, Y., Häussler, M., Li, Z., Lam, J. W. Y., Dong, Y., Sung, H. H.-Y., Williams, I. D. and Tang, B. Z., "Protein detection and quantitation by tetraphenylethene-based fluorescent probes with aggregation-induced emission characteristics," *J. Phys. Chem. B* 111(40), 11817-11823 (2007).
- [28] Yuan, W. Z., Zhao, H., Shen, X. Y., Mahtab, F., Lam, J. W. Y., Sun, J. Z. and Tang, B. Z., "Luminogenic polyacetylenes and conjugated polyelectrolytes: synthesis, hybridization with carbon nanotubes, aggregation-induced emission, superamplification in emission quenching by explosives, and fluorescent assay for protein quantitation," *Macromolecules* 42(24), 9400-9411 (2009).
- [29] Kolb, H. C., Finn, M. G., Sharpless, K. B., "Click chemistry: diverse chemical function from a few good reactions," *Angew Chem. Int. Ed.* 40(11), 2004-2021 (2001).
- [30] Lodge, T. P., "A virtual issue of macromolecules: 'click chemistry in macromolecular science,'" *Macromolecules* 42(12), 3827-3829 (2009) and reference therein.
- [31] Binder, W. H., Sachsenhofer, R. *Macromol. Rapid Commun.*, "'Click' chemistry in polymer and material science: An update," 29(12-13), 952-981 (2008).
- [32] Gujadhur, R., Venkataraman, D. and Kintigh, J. T., "Formation of aryl-nitrogen bonds using a soluble copper(I) catalyst," *Tetrahedron Lett.* 42(29), 4791-4793 (2001).
- [33] Qin, A., Lam, J. W. Y., Jim, C. K. W., Zhang, L., Yan, J., Häussler, M., Liu, J., Dong, Y., Liang, D., Chen, E., Jia, G. and Tang, B. Z., "Hyperbranched polytriazoles: Click polymerization, regioisomeric structure, light emission, and fluorescent patterning," *Macromolecules* 41(11), 3808-3822 (2008).
- [34] Brandrup, J., Immergut, E. H. and Grulke, E. A., Eds., "Polymer Handbook, 4th Ed.," Wiley: New York (1999).
- [35] Gray, G. W. and Goodby, J. W. G., "Smectic Liquid Crystals: Texture and Structures," Leonard Hill: London (1984).
- [36] Ye, C., Zhang, H.-L., Huang, Y., Chen, E.-Q., Lu, Y., Shen, D., Wan, X.-H., Shen, Z., Cheng, S. Z. D. and Zhou, Q.-F., "Molecular weight dependence of phase structures and transitions of mesogen-jacketed liquid crystalline polymers based on 2-vinylterephthalic acids," *Macromolecules* 37(19), 7188-7196 (2004).
- [37] Yoon, Y., Ho, R.M., Li, F. M., Leland, M. E., Park, J. Y., Cheng, S. Z. D., Percec, V. and Chu, P. "Existence of highly ordered smectic structures in a series of main-chain liquid-crystalline polyethers," *Prog. Polym. Sci.* 22(4), 765-794(1997).